IEEE Photonics Journal
An IEEE Photonics Society Publication

Open Access

High-Efficiency Photonic Microwave Downconversion With Full-Frequency-Range Coverage

Volume 7, Number 4, August 2015

Peixuan Li
Wei Pan
Xihua Zou
Shilong Pan
Bin Luo
Lianshan Yan

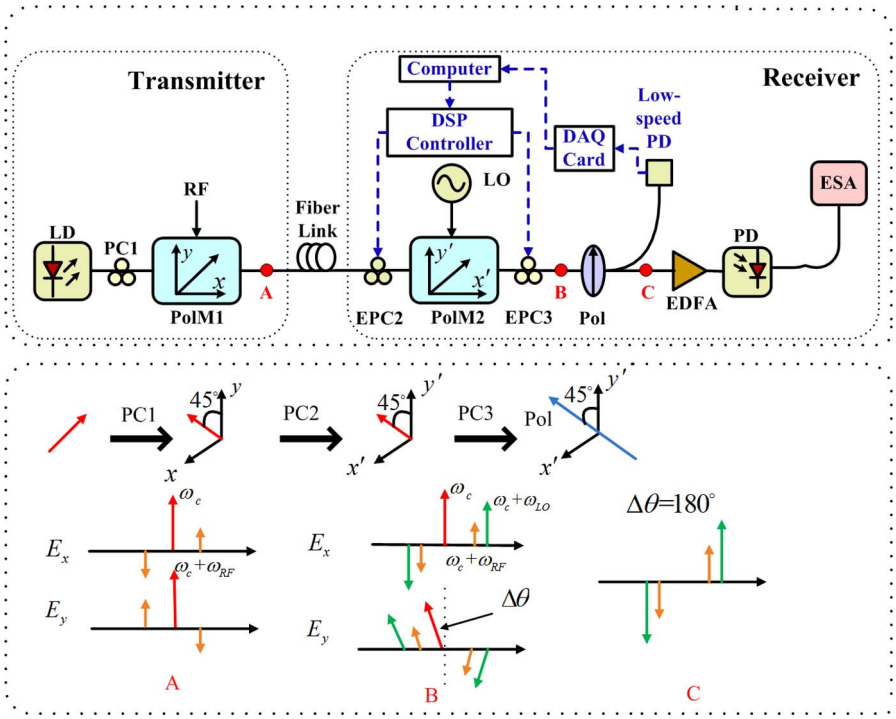

DOI: 10.1109/JPHOT.2015.2448522

High-Efficiency Photonic Microwave Downconversion With Full-Frequency-Range Coverage

Peixuan Li,[1] Wei Pan,[1] Xihua Zou,[1] Shilong Pan,[2] Bin Luo,[1] and Lianshan Yan[1]

[1]Center for Information Photonics and Communications, School of Information Science and Technology, Southwest Jiaotong University, Chengdu 610031, China
[2]Key Laboratory of Radar Imaging and Microwave Photonics, Ministry of Education, Nanjing University of Aeronautics and Astronautics, Nanjing 210016, China

DOI: 10.1109/JPHOT.2015.2448522

Manuscript received May 12, 2015; revised June 17, 2015; accepted June 19, 2015. Date of current version July 3, 2015. This work was supported in part by the Research Fund for the Doctoral Program of Higher Education of China under Grant 20110184130003, by the National Natural Science Foundation of China under Grant 61378008, by the "973" Project under Grant 2012CB315704, and by the Program for New Century Excellent Talents in University of China under Grant NCET-12-0940.
Corresponding author: X. Zou (e-mail: zouxihua@swjtu.edu.cn).

Abstract: Microwave frequency downconversion is optically implemented by using two cascaded polarization modulators (PolMs), characterized by full-frequency-range coverage and high conversion efficiency. In this proposed approach, the incident radio-frequency signal (RF) and the local oscillator signal (LO) are applied to the first PolM at the transmitter and the second one at the receiver, respectively. Effective optical carrier suppression can be achieved using the cascaded PolMs, whereas the optical sidebands induced by the RF and the LO signals remain unchanged. Since no additional optical filter is needed, the lower operation frequency limit in other approaches with an optical filter is eliminated, such that a full-frequency-range coverage is ensured in this approach. Meanwhile, the use of optical carrier suppression (OCS) enables high conversion efficiency for microwave downconversion. In the proof-of-concept experiments, the conversion efficiency is improved by over 20 dB within the frequency range from 2 to 15 GHz, as compared to those of cascaded modulators without OCS. Both the upper and the lower limits of such a frequency range can be greatly extended when test instruments with full frequency range are used.

Index Terms: Microwave photonics, optical frequency conversion, optical carrier suppression (OCS), high conversion efficiency, full frequency range, polarization modulation.

1. Introduction

For many applications such as electronic warfare, communication, remote sensing, and radar, it is of critical importance to downconvert a high-frequency microwave signal to a low-frequency or intermediate-frequency (IF) one at the receiver to reduce frequency-bandwidth requirement and enhance the dynamic range. Compared with the downconversion implemented by conventional electrical mixer, microwave photonic mixer (MPM) is characterized by high isolation, low loss, wide bandwidth, and immunity to the electromagnetic interference (EMI). Therefore, MPM has been considered as an alternative to satisfy the demand of application scenarios with high operation frequency such as radio-over-fiber (ROF) systems, microwave receivers, and radars.

Several cascaded Mach–Zehnder modulator (MZMs) structures were proposed to implement MPM [1]–[3]. In these structures, high isolation between the radio-frequency (RF) signal port and the local oscillator (LO) signal port was obtained, and special applications such as Doppler frequency shift estimation are realized [4]. On the other hand, they might have low conversion efficiency which is defined as the ratio between the IF output power to the RF input power [7]. In general, due to the limited saturated input optical power of photodetectors (PDs), the conversion efficiency cannot be infinitely improved by increasing the incident optical power, as most of the average power is contributed by the optical carrier. Since the IF output power is mainly determined by the optical sidebands induced by the RF and the LO signals, a number of MPM approaches with improved conversion efficiency using optical carrier suppression (OCS) were proposed [5]–[9]. Nonlinear effect used in [5] may increase nonlinearity of the system. Dual-parallel MZM (DPMZM) and Sagnac loop interferometer structures are used to achieve OCS and high-amplitude sidebands induced by RF and LO signals in [6] and [7]. MPM using OCS is implemented in [8] by connecting an optical filter at the output of two cascaded phase modulators (PM). The optical filter needed should have critically stable center wavelength, extremely narrow stopband and transmission band, and high rejection ratio simultaneously. To some extent, the operation frequency range is still limited, especially for the low-frequency range, owing to the effective stopband of currently available narrow optical filters. In [9], the optical filter was replaced by the SBS-based OCS technique. Here, an additional wideband frequency-shift module and amplification devices may make this scheme complex [10].

In this paper, we propose a novel photonic approach to implement microwave frequency downconversion using two cascaded polarization modulators (PolMs). High-performance OCS can be easily achieved by adjusting the polarization controllers (PCs) placed before and after the second PolM driven by the LO signal without any additional optical filter. In this approach, the limitation of lower operation frequency can be eliminated, and high-performance OCS is realized. In proof-of-concept experiments, the optical sidebands induced by the LO signal are about 20 dB beyond the optical carrier, and an over 20 dB improvement to the conversion efficiency is obtained, compared with that of the conventional microwave downconverter based on cascaded MZMs structures within the frequency range from 2 to 15 GHz. In addition, if the test instruments with full frequency range are used in the experiments, both the upper and the lower limits of the operation frequency range can be greatly extended.

2. Principle

The schematic diagram of the proposed approach is shown in Fig. 1(a). The light wave from a laser diode (LD) is oriented at an angle of 45° to one principal axis of PolM1 at the transmitter. The PolM is a special phase modulator that supports both transverse-electric (TE) and transverse-magnetic (TM) modes with opposite phase modulation indices [11]. When the RF signal with angular frequency ω_{RF} is applied to PolM1, the output electrical fields of two orthogonal directions of PolM1 can be expressed as

$$\begin{bmatrix} E_x \\ E_y \end{bmatrix} = \frac{\sqrt{2}}{2} E_{in} \begin{bmatrix} e^{j\omega_c t} e^{j\beta_1 \cos\omega_{\mathrm{RF}} t} \\ e^{j\omega_c t} e^{-j\beta_1 \cos\omega_{\mathrm{RF}} t} \end{bmatrix} \tag{1}$$

where E_{in} and ω_c are the amplitude and the angular frequency of the optical carrier, $\beta_1 = \pi \cdot (V_{\mathrm{RF}}/V_{\pi 1})$ is the modulation index of PolM1, V_{RF} is related to the amplitude of the input RF signal, and $V_{\pi 1}$ is the half-wave voltage of PolM1. Then, the modulated light wave is sent to remotely or locally located receiver through a fiber link.

After transmission in the fiber link, we can align two principal axes of PolM2 with those of PolM1 by using PC2. By applying the LO signal at ω_{LO} to PolM2, the electrical fields of two orthogonal directions at the output of PolM2 can be written as

$$\begin{bmatrix} E_{x'} \\ E_{y'} \end{bmatrix} = \begin{bmatrix} E_x e^{j\beta_2 \cos\omega_{\mathrm{LO}} t} \\ E_y e^{-j\beta_2 \cos\omega_{\mathrm{LO}} t} e^{j\Delta\theta} \end{bmatrix} \tag{2}$$

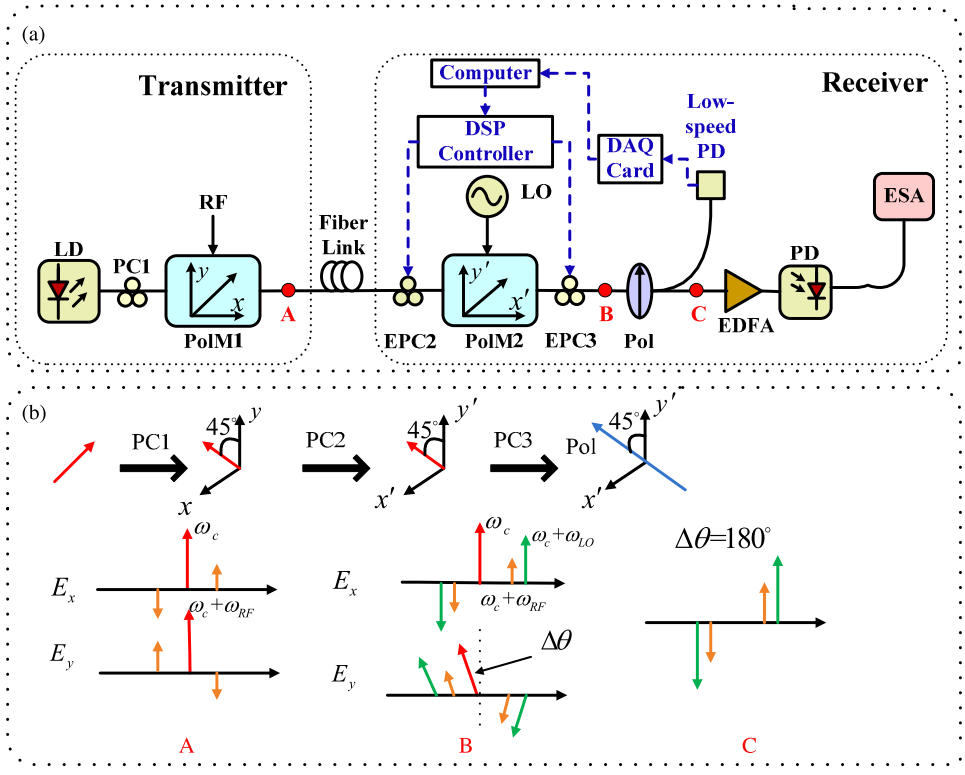

Fig. 1. (a) Schematic of the proposed photonic-assisted microwave frequency mixer. (b) Evolution of the polarization directions of light and optical spectra at different points. LD: laser diode; PC: polarization controller; PolM: polarization modulator; Pol: polarizer; EDFA: erbium-doped fiber amplifier; PD: photodetector; ESA: electrical spectrum analyzer. EPC: electrical controlled PC; DAQ: data acquisition; DSP: digital signal processing.

where E_x and E_y are the output electrical fields of two orthogonal directions of PolM1, $\beta_2 = \pi \cdot (V_{LO}/V_{\pi 2})$ is the modulation index of PolM2, V_{LO} is related to the amplitude of input LO signal, and $V_{\pi 2}$ is the half-wave voltage of PolM2, $\Delta\theta$ is the static phase difference between $E_{x'}$ and $E_{y'}$ introduced by PC3. Based on the Jacobi–Anger expansion, (2) can be expressed as [18]

$$\begin{bmatrix} E_{x'} \\ E_{y'} \end{bmatrix} \approx \frac{\sqrt{2}}{2} E_{in} \begin{bmatrix} e^{j\omega_c t} \cdot \sum_{n=-\infty}^{\infty} \sum_{m=-\infty}^{\infty} j^{n+m} J_n(\beta_1) J_m(\beta_2) \exp[j(n\omega_{RF} t + m\omega_{LO} t)] \\ e^{j\omega_c t} e^{j\Delta\theta} \sum_{n=-\infty}^{\infty} \sum_{m=-\infty}^{\infty} j^{n+m} J_n(\beta_1) J_m(\beta_2) \exp\{j[n\omega_{RF} t + m\omega_{LO} t + \pi(n+m)]\} \end{bmatrix} \tag{3}$$

where $J_n(\cdot)$ is the nth-order Bessel function of the first kind, and n and m are integers. When the amplitude of the RF signal is much lower than that of the LO signal, under small signal modulation, only five largest terms are considered such that (3) can be simplified as

$$\begin{bmatrix} E_{x'} \\ E_{y'} \end{bmatrix} \approx \frac{\sqrt{2}}{2} E_{in} \begin{bmatrix} e^{j\omega_c t}\left(J_{01}J_{02} + J_{02}J_{11}e^{j\left(\omega_{RF} t+\frac{\pi}{2}\right)} - J_{02}J_{11}e^{-j\left(\omega_{RF} t+\frac{\pi}{2}\right)}\right. \\ \left. + J_{01}J_{12}e^{j\left(\omega_{LO} t+\frac{\pi}{2}\right)} - J_{01}J_{12}e^{-j\left(\omega_{LO} t+\frac{\pi}{2}\right)}\right) \\ e^{j\omega_c t}e^{j\Delta\theta}\left(J_{01}J_{02} - J_{02}J_{11}e^{j\left(\omega_{RF} t+\frac{\pi}{2}\right)} + J_{02}J_{11}e^{-j\left(\omega_{RF} t+\frac{\pi}{2}\right)}\right. \\ \left. - J_{01}J_{12}e^{j\left(\omega_{LO} t+\frac{\pi}{2}\right)} + J_{01}J_{12}e^{-j\left(\omega_{LO} t+\frac{\pi}{2}\right)}\right) \end{bmatrix} \tag{4}$$

where $J_{kr} = J_k(\beta_r)$, β_r $(r = 1, 2)$ are the modulation indices of PolM. The remodulated optical signal is then sent to a polarizer with its principal axis oriented at an angle of 45° to one

principal axis of PolM2. When $\Delta\theta = 180^\circ$, the combined electrical field at the output of the polarizer is

$$E_c = \frac{\sqrt{2}}{2}E_{x'} + \frac{\sqrt{2}}{2}E_{y'} \approx E_{in}(J_{02}J_{11}\left(e^{j\left(\omega_c t+\omega_{RF}t+\frac{\pi}{2}\right)} - e^{j\left(\omega_c t-\omega_{RF}t-\frac{\pi}{2}\right)}\right) + J_{01}J_{12}\left(e^{j\left(\omega_c t+\omega_{LO}t+\frac{\pi}{2}\right)} - e^{j\left(\omega_c t-\omega_{LO}t-\frac{\pi}{2}\right)}\right). \quad (5)$$

From (5), it is obvious that high-performance OSC can be easily obtained by simply adjusting PC2 and PC3 without any optical filter, while the amplitude of sidebands induced the RF and LO signals remain unchanged. For a clear description, the evolution of the polarization directions of the light waves and the corresponding optical spectra at different points are illustrated in Fig. 1(b). We adjust PC2 to align the two principal axes of PolM2 with those of PolM1, wherein the optical carrier is modulated by both RF and LO signals in two orthogonal modes (TE and TM modes) with opposite phase modulation indices. The corresponding optical spectra measured at point B are shown in Fig. 1(b). Here, PolM2 in conjunction with PC3 and the polarizer is equivalent to an intensity modulator, of which the transmission point can be changed by tuning PC3 [11]. As the equivalent intensity modulator is biased at the minimum transmission point (MITP) (i.e., $\Delta\theta = 180^\circ$), the optical carrier is eliminated and only the first-order sidebands induced by the RF and the LO signals are generated.

The Erbium-doped fiber amplifier (EDFA) located after the polarizer is used to amplify the sidebands induced by the RF and the LO signals. The amplified optical signal is sent to the PD to generate the desired IF signal. Consequently, the obtained IF signal with angular frequency of $\omega_{LO} - \omega_{RF}$ can be expressed as

$$I_{IF}(t) \propto 2RP_{in}T_mJ_{01}J_{02}J_{11}J_{12}\cos(\omega_{LO} - \omega_{RF}) \quad (6)$$

where $P_{in} = |E_{in}|^2$ is proportional to the power of optical carrier, T_m represents the total gain or the loss of optical link, and R is the responsivity of the PD. Thus, for a PD with limited saturated input optical power, the elimination of optical carrier would be beneficial for transferring more power to the sidebands induced by the RF and the LO signals, which will result in a higher power level for the IF signal. On the other hand, because an optical filter in [8] is no longer needed here, the limitation of operation frequency range can be effectively overcome. Therefore, without additional optical filter, we can realize photonic microwave frequency downconversion with full frequency range coverage and high conversion efficiency in this structure. In addition, unlike the schemes in [6] and [7], the cascaded modulators in this proposed approach will permit the RF receiver to be placed at a remote location away from the transmitter, which might available for some applications with remote ports in ROF or electronic warfare systems. In addition, to fully investigate the performance of the proposed mixer, a comparison among the specifications of the proposed mixer based on dual-cascaded PolMs (CPolMs) and the conventional dual-cascaded MZMs (CMZMs) has been carried out via simulations using commercial software VPItransmissionMaker, when the modulation indices of LO signals were optimized for the maximum conversion efficiency. Based on the definition about these specifications given in [14] and [17], the results are listed in Table I. The noise floor of our proposal is higher than that of the conventional CMZMs based mixer. Benefiting from the improvement of conversion efficiency, the CPolMs based mixer got an improvement in the spurious free dynamic range (SFDR) and noise figure (NF) compared with the CMZMs based mixer.

3. Experiments and Discussions

To verify the proposed approach, experiments based on the setup shown in Fig. 1(a) are performed. The optical carrier at 1549.15 nm is emitted from a tunable laser with a narrow linewidth of 1 kHz. The light wave is then modulated by an RF signal in PolM1 which has a 3-dB bandwidth of 40 GHz and a half-wave voltage of 3.5 V at the transmitter. After transmission through a section of fiber link, at the receiver, PolM2 with a half-wave voltage of 5.3 V is

TABLE I

Performance comparison of two different structures based mixers

	CPolMs	CMZMs
Conversion efficiency	-17.27 dB	-39 dB
3rd-order intercept point,	27 dBm	32.5 dBm
Noise floor	-156 dBm	-163 dBm
Noise figure	35.2 dB	50 dB
SFDR	110.53 $dBHz^{2/3}$	104.33 $dBHz^{2/3}$

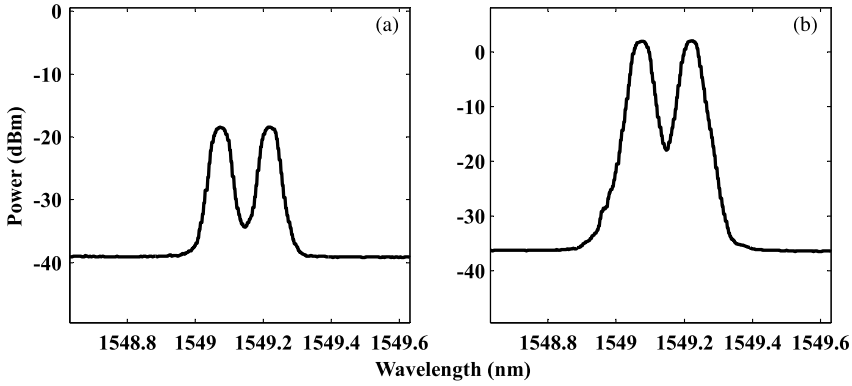

Fig. 2. Measured optical spectra before PD without (a) and with (b) LO signal applied.

connected to PolM1 and driven by the strong LO signal. An EDFA is then used to amplify the optical signal. Finally, the amplified signal is sent to a PD to generate the IF signal.

To achieve a high conversion efficiency, we adjust the PCs placed before and after PolM2 to implement OCS. While in practice, the state of polarization (SOP) of light is sensitive to the environment such as stress, temperature and so on. Therefore, an accurate adjustment of the SOPs is deeply needed in microwave photonics systems, as well as high-capacity polarization-division-multiplexing systems. Fortunately, several automatic control schemes realized by feedback systems were proposed in [12] and [13] to stabilize or to trace the SOP of light. Therefore it is believed that these automatic control schemes can be used in our photonic downconversion approach in practice, while in our proof-of-concept experiment polarization controllers (PCs) were used to adjust the SOP of light. Here, one promising solution to solve the problem presented above is shown in Fig. 1(a), where a slight proportion of the light is sent to a similar feedback control circuit to automatically control the SOP of light.

A 9.05-GHz RF signal with a power level of -9 dBm is firstly applied to PolM1, while an LO signal at 9.152 GHz with a power level of 10 dBm is applied to PolM2. The measured optical spectra without and with the LO signal are demonstrated in Fig. 2(a) and (b). When the LO modulator is absent, we have $\beta_2 = 0$, $J_{02} = 1$, and $J_{12} = 0$. Therefore, only the terms of first-order sidebands induced by RF signal are observed in (5), which agrees well with the result shown in Fig. 2(a). It is clear that the power level of each sideband induced by the RF and the LO signals is greater than that of the optical carrier. In detail, a suppression ratio of 20 dB between the optical carrier and the sideband induced by LO signal is observed in Fig. 2(b), which is as high as that in [7]. By setting the gain of the EDFA, the amplified optical signal with a 10-dBm power is

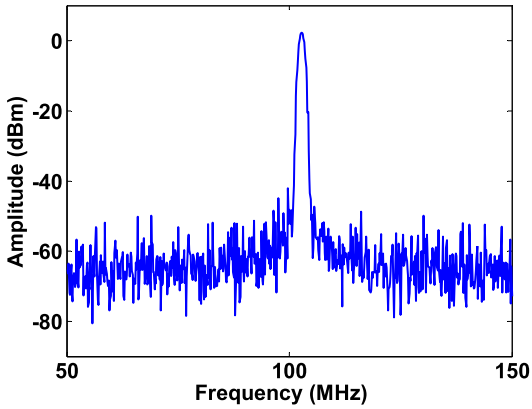

Fig. 3. Measured electrical spectrum of the IF signal at 102 MHz.

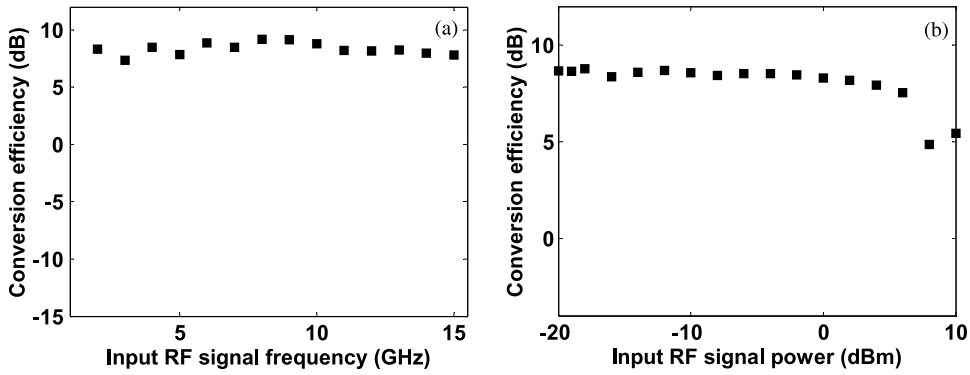

Fig. 4. (a) Conversion efficiency as an function of input RF signal frequency. (b) Conversion efficiency as an function of input RF signal power.

sent to PD for generating the IF signal. The measured spectrum of the generated IF signal at 102 MHz is shown in Fig. 3.

From the result shown in Fig. 3, the power level of the generated IF signal is 0.25 dBm as an input RF signal of -9 dBm is received. Thus, the conversion efficiency is estimated as 9.25 dB, indicating an improvement over 20 dB, as compared with that in conventional cascaded MZMs structure [9]. To get more details, the conversion efficiency is tested for different frequencies and different power levels of the input RF signal, as shown in Fig. 4(a). Within the frequency range from 2 to 15 GHz, the fluctuation of the conversion efficiency is less than ± 0.8 dB. The 1 dB compression point is defined by the point at which the power of IF signal deviates by 1 dB from the small signal linear response for the input power of RF signal [15]. Since the conversion efficiency is determined by the difference between the powers of the RF and IF signals, in dB units, the 1 dB compression point can be concluded as the point that the conversion efficiency drops by 1 dB, and it is estimated to be 6 dBm from Fig. 4(b) in the experiment.

It should be noticed that, although the experimental results demonstrate a frequency range of $2 \sim 15$ GHz. Here, the lower frequency limit is mainly limited by the minimum output frequency of the used microwave generator (Anritsu MG3694B) at 2 GHz, and the upper frequency limit is limited by the operation bandwidth of the optical and the electrical devices employed in the experiment. Thus, if the test instruments used in the experiments have a full frequency range, the lower and the upper limits of the operation frequency range of the proposed approach can be greatly improved. For instance, the operation frequency here can be as low as tens of megahertz and beyond 40 GHz. Therefore, from the results shown in Fig. 4(a), the limitation to low-frequency

operation in [8] is removed, such that a full frequency range coverage and a high conversion efficiency are realized simultaneously in the proposed approach.

4. Conclusion

A photonic approach was proposed to perform microwave frequency downconversion with full frequency range coverage and high conversion efficiency. In the proof-of-concept experiments, without the optical filtering technique, the generated IF signal with high power, resulting from the high-performance OCS, was observed. An over 20-dB improvement to the conversion efficiency within the frequency range from 2 to 15 GHz was obtained, compared with that of the conventional microwave downconverter based on cascaded MZMs structures. Such a frequency range can be extended to a full frequency-range coverage in the proposed approach.

References

[1] G. K. Gopalakrishnan, W. K. Burns, and C. H. Bulmer, "Microwave-optical mixing in Limo3 modulators," *IEEE Trans. Microw. Theory Tech.*, vol. 41, no. 12, pp. 2383–2391, Dec. 1993.
[2] C. K. Sun, R. J. Orazi, S. A. Pappert, and W. K. Bums, "A photonic-link millimeter-wave mixer using cascaded optical modulators and harmonic carrier generation," *IEEE Photon. Technol. Lett.*, vol. 8, no. 9, pp. 1166–1168, Sep. 1996.
[3] H. Chi and J. P. Yao, "Frequency quadrupling and upconversion in a radio over fiber link," *IEEE Photon. Technol. Lett.*, vol. 26, no. 15, pp. 2706–2711, Aug. 2008.
[4] X. H. Zou *et al.*, "Photonic approach to wide-frequency-range high-resolution microwave/millimeter-wave Doppler frequency shift estimation," *IEEE Trans. Microw. Theory Tech.*, vol. 63, no. 4, pp. 1421–1430, Apr. 2015.
[5] H. J. Song and J. I. Song, "Simultaneous all-optical frequency downconversion technique utilizing an SOA-MZI for WDM Radio over Fiber (RoF) applications," *J. Lightw. Technol.*, vol. 24, no. 8, pp. 3028–3034, Aug. 2006.
[6] Y. S. Gao *et al.*, "An efficient photonic mixer with frequency doubling based on a dual-parallel MZM," *Opt. Commun.*, vol. 321, no. 15, pp. 11–15, Jun. 2014.
[7] E. H. W. Chan and R. A. Minasian, "Microwave photonic downconversion using phase modulators in a Sagnac loop interferometer," *IEEE J. Sel. Top. Quantum Electron.*, vol. 19, no. 6, Nov.–Dec. 2013, Art ID. 3500208.
[8] V. R. Pagan, B. M. Haas, and T. E. Murphy, "Linearized electrooptic microwave downconversion using phase modulation and optical filtering," *Opt. Express*, vol. 19, no. 2, pp. 883–895, Jan. 2011.
[9] E. H. W. Chan and R. A. Minasian, "High conversion efficiency microwave photonic mixer based on stimulated Brillouin scattering carrier suppression technique," *Opt. Lett.*, vol. 38, no. 24, pp. 5292–5295, Dec. 2013.
[10] W. Li, L. X. Wang, and N. H. Zhu, "All-optical microwave photonic single-passband filter based on polarization control through stimulated Brillouin scattering," *IEEE Photon. J.*, vol. 5, no. 4, Aug. 2013, Art ID. 5501411.
[11] S. L. Pan and J. P. Yao, "Optical clock recovery using a polarization-modulator-based frequency-doubling optoelectronic oscillator," *J. Lightw. Technol.*, vol. 27, no. 16, pp. 3531–3539, Aug. 2009.
[12] M. Martinelli, P. Martelli, and S. M. Pietralunga, "Polarization stabilization in optical communications systems," *J. Lightw. Technol.*, vol. 24, no. 11, pp. 4172–4183, Nov. 2006.
[13] X. S. Yao, L. S. Yan, B. Zhang, A. E. Willner, and J. F. Jiang, "All-optic scheme for automatic polarization division demultiplexing," *Opt. Express*, vol. 15, no. 12, pp. 7407–7414, Jun. 2007
[14] L. Liu, S. L. Zheng, X. M. Zhang, X. F. Jin, and H. Chi, "Performances improvement in radio over fiber link through carrier suppression using stimulated Brillouin scattering," *Opt. Express.*, vol. 18, no. 11, pp. 11827–11837, May 2010.
[15] B. H. Kolner and D. W. Dolfi, "Intermodulation distortion and compression in an integrated electrooptic modulator," *Appl. Opt.*, vol. 26, pp. 3676–3680, Sep. 1987.
[16] E. H. W. Chan and R. A. Minasian, "Microwave photonic downconverter with high conversion efficiency," *J. Lightw. Technol.*, vol. 30, no. 23, pp. 4172–4183, Dec. 2012.
[17] C. H. Cox, *Analog Optical Links; Theory and Practice*. Cambridge, U.K.: Cambridge Univ. Press, 2004, pp. 159–262.
[18] H. Chi, X. H. Zou, and J. P. Yao, "Analytical models for phase-modulation-based microwave photonic systems with phase modulation to intensity modulation conversion using a dispersive device," *J. Lightw. Technol.*, vol. 27, no. 5, pp. 511–521, Mar. 2009.